**Structural Engineering and Mechanics**, *Vol. 67, No. 3 (2018) 245-254*
DOI: https://doi.org/10.12989/sem.2018.67.3.245


# Structural damage identification using cloud model based fruit fly optimization algorithm

Tongyi Zheng[1], Jike Liu[1], Weili Luo*[2] and Zhongrong Lu[1]

[1]*Department of Applied Mechanics, Sun Yat-Sen University, Guangzhou, P.R. China*
[2]*School of Civil Engineering, Guangzhou University, Guangzhou, P.R. China*

*(Received March 30, 2018, Revised May 14, 2018, Accepted May 15, 2018)*

**Abstract.** In this paper, a Cloud Model based Fruit Fly Optimization Algorithm (CMFOA) is presented for structural damage identification, which is a global optimization algorithm inspired by the foraging behavior of fruit fly swarm. It is assumed that damage only leads to the decrease in elementary stiffness. The differences on time-domain structural acceleration data are used to construct the objective function, which transforms the damaged identification problem of a structure into an optimization problem. The effectiveness, efficiency and accuracy of the CMFOA are demonstrated by two different numerical simulation structures, including a simply supported beam and a cantilevered plate. Numerical results show that the CMFOA has a better capacity for structural damage identification than the basic Fruit Fly Optimization Algorithm (FOA) and the CMFOA is not sensitive to measurement noise.

**Keywords:** damage identification; swarm intelligence; cloud model; fruit fly optimization algorithm; time domain data

## 1. Introduction

Damage identification of structures has received wide attentions and has well developed in the last few decades (Bakhtiari-Nejad *et al.* 2005, Hosseinzadeh *et al.* 2015, Li *et al.* 2016, Teixeira *et al.* 2016, Zhu *et al.* 2014). Using this method, deterioration in the physical properties of important structures (such as super-tall buildings (Wei 2011) and long suspension bridges (Sun *et al.* 2014, Wang and Ni 2015)) can be detected. The identified parameters can be used for the assessments of serviceability and stability of the structures.

A great number of approaches have been proposed for detecting structural damage, among which the most common approaches are those gradient-based methods in either frequency domain (Cao *et al.* 2011, Kim *et al.* 2003, Xia *et al.* 2002) or time domain (Gao and Lu 2009, Li *et al.* 2015, Zhang *et al.* 2007). However, their formulations and implementations are complex, especially when second-order derivatives are needed to be computed. Alternatively, many identification methods have been put forward based on the swarm intelligent optimization, such as genetic algorithm (GA) (Nobahari *et al.* 2017), artificial bee colony optimization (ABC) (Ding *et al.* 2016, Sun *et al.* 2013, Xu *et al.* 2015), ant colony optimization (ACO) (Daei and Mirmohammadi 2015, Majumdar *et al.* 2014), artificial immune syst. (AIS) (Patel *et al.* 2011), particle swarm optimization (PSO) (Saada *et al.* 2013) and artificial fish swarm algorithm (AFSA) (Guo 2015). For example, a modified ABC was studied by Sun *et al.* (2013) to identify two linear systems (5-DOF and 20-DOF) and a nonlinear system (2-DOF) with full and partial measurements under noise free and noise polluted situations. Saada *et al.* (2013) proposed an improved PSO to predict the damage location and extent of beam structures through experimentally determined natural frequencies.

More recently, a new swarm intelligent optimization algorithm, Fruit Fly Optimization Algorithm (FOA), was proposed in 2011, which was inspired by the foraging behavior of fruit fly swam living in the tropical climate zones (Pan 2011). The FOA has many merits such as ease of implementation and fast convergence rate, and thus has been successfully applied in solving a wide range of optimization problems, such as the solution of financial distress model (Pan 2012) and the prediction of annual power load (Chen *et al.* 2013). During recent several years, some improvements of the FOA have been made to enhance its effectiveness and global convergence ability. For example, a modified fruit fly optimization algorithm (MFOA) (Pan 2013) was proposed by the introduction of an escape parameter for overcoming its deficiency of non-negative fitness function. For avoiding being trapped in local optimal solutions, a multi-swarm fruit fly optimization (MSFOA) (Yuan *et al.* 2014) was reported by the adoption of multi-swarm strategy techniques. For eliminating the disadvantages of fixed values of search radius of FOA, Pan *et al.* (2014) proposed an improved fruit fly optimization (IFFO) by the introduction a new control parameter that varies with iterations. The most recent improvement has been carried out by Wu *et al.* (2015) in 2015. In that paper, a CMFOA was proposed by the introduction of a normal cloud generator and an adaptive parameter strategy. The former aimed to improve the convergence performance of FOA, and the latter was to enhance the global search ability and the accuracy of the solution. Numerical results of 33 benchmark functions confirmed that the CMFOA was able

*Corresponding author, Assistant Professor
E-mail: wlluo@gzhu.edu.cn



ISSN: 1225-4568 (Print), 1598-6217 (Online)

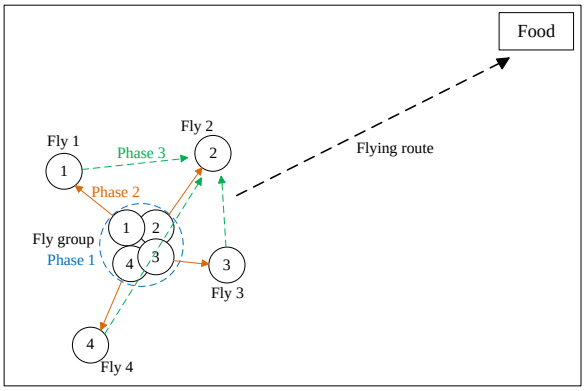


Fig. 1 Food foraging behavior of fruit fly swarm

to obtain better or competitive performance compared with other variants of FOA (including MFOA, MSFOA and IFFO) and seven state-of-the-arts swarm intelligent optimization algorithms.

However, the FOA and its variants have been seldom reported for applications in structural damage identification. Quite recently, Li and Lu (2015) successfully employed the MSFOA for the detection of damages in a beam, a truss, and a discrete spring-mass system by using natural frequencies and mode shapes for establishing objective function. In that paper, two deficiencies are worth pointing out: (a) natural frequencies are easily affected by environmental factors (such as temperature), and mode shapes are quite difficult to be accurately measured; (b) the damage identification method based on MSFOA is sensitive to measurement noise (Li and Lu 2015). In this paper, the most advanced FOA variant, CMFOA, is applied for the identification of structural damage, which has been proved to possess better global convergence ability compared with other variants of the FOA (Wu and Zhang 2015). Instead of using frequency domain modal data, this paper adopts time domain observed data for establishing objective function, in which less sensors are required and time domain data are sensitive to structural damages even a local damage. To evaluate the effectiveness and accuracy of the damage identification method using CMFOA, two numerical examples, including a simply supported beam and a cantilevered plate, are studied and their results are compared with those computed by the method using the basic FOA. The influence of different levels of artificial noise are also considered.

The paper is organized as follows. Section 2 introduces the CMFOA and the damage parameter to construct objected function. Section 3 presents the implementation of structural damage identification using the CMFOA. Numerical examples are given in Section 4. Finally, conclusions are drawn in Section 5.

## 2. Methodology

### *2.1 Fruit fly optimization algorithm*

#### *2.1.1 Basic fruit fly algorithm*

FOA is a global optimization algorithm based on food searching characteristics of fruit fly swarm. Compared with other species, fruit fly possesses better sensing and perception especially in olfactory and vision. To forage a food source, fruit fly firstly utilizes olfactory to catch even a faint odor from the air and then approaches to the food, and secondly employs its sensitive vision to fly directly to the food source or the company's flocking location. FOA can be divided into three phases: initialization of the problem parameters, osphresis foraging phase and vision foraging phase (Pan 2011). Fig. 1 shows the food searching procedure of fruit fly swarm.

Phase 1: Initialization of the problem parameters

This phase aims to initiate parameters of FOA, including the maximum iterative number $Iter_{max}$, the fruit fly swarm population $N$, and the fruit fly swarm location $X\_axis_j$. Fixed values are usually assigned for the former two variables, and it is a common practice to randomly initialize $X\_axis_j$ in the search space as follows

$$X\_axis_j = rand(\,) \times \left(U_{bj} - L_{bj}\right) + L_{bj}, j = 1,2,\dots,n \tag{1}$$

where *rand( )* is a random function which returns a value from the uniform distribution on the interval [0,1]; $n$ is the number of swarms, representing the number of decision variables; $U_{bj}$ and $L_{bj}$ are upper and lower bounds of fruit fly swarm location for the decision variable, respectively.

Phase 2: Osphresis foraging phase

In this phase, a population of $N$ food sources is generated randomly around the current fruit fly swarm position. Define $X_{ij}$ as the new random location and distance of the $i$-th fruit fly in the $j$-th swarm and its equation is a uniformly distributed random function and is given as follows

$$X_{ij} = X\_axis_j + randValue, i = 1,2,\dots,N;\ j = 1,2,\dots,n \tag{2}$$

Phase 3: Vision foraging phase

In this phase, a greedy selection procedure is carried out and the best individual with the minimum fitness, $X_{best}$, is firstly found out among the fruit fly swarm. If fitness function $f(X_{best})$ is better than the value at the present swarm location $f(X\_axis_j)$, $X\_axis_j$ is updated with $X_{best}$

$$X\_axis_j = X_{best}, if\ f(X_{best}) < f(X\_axis_j), j = 1,2,\dots,n \tag{3}$$

This represents fruit fly swarm flying towards the new location using vision.

Both osphresis and vision foraging phases are repeated until the iterative number reaches the maximum iterative number $Iter_{max}$.

#### *2.1.2 Cloud model based fruit fly optimization algorithm*

The basic FOA adopts the uniformly distributed random function, Eq. (2), to yield new locations for each fruit fly during the osphresis searching phase. This ignores various judgments and fly routines for different fruit flies. To take this randomness and fuzziness feature into consideration, the normal cloud generator was introduced to generate new locations as follows (Wu and Zhang 2015)

$$X_{ij} = \begin{cases} C_x\left(X_{axis\,j}, En, , He\right), if\ j = d \\ X\_axis_j, \qquad\quad otherwise \end{cases}, j = 1,2,\ldots,n \tag{4}$$

where $d$ is a random integer in the range of [1, $n$]; $En$ (Entropy) represents the search radius; $He$ (Hyper Entropy) stands for the stability of the search.

The fruit fly swarm location in the early search stage is usually far away from the optimum solution, and a large range of search radius is required. However, with the evolution of the swarm, its location is close to the optimum solution, so a small search radius is appropriate to fine the solutions in the last stage. Thus, to balance the abilities of exploration and exploitation, an adaptive strategy of $En$ and $He$ that dynamically varies with iterations is adopted as the follows (Wu and Zhang 2015)

$$En = En\_\max \times \left(1 - \frac{Iter}{Iter_{max}}\right)^c \tag{5}$$

$$He = 0.1En \tag{6}$$

where $En\_\max = (U_b - L_b)/4$ is the maximum search radius; $c$ is a positive integer and stands for the exploitation accuracy over the iterations. A larger $c$ implies faster and more accurate exploitation.

### *2.2 Parameterization of structure damage*

#### *2.2.1 Governing equation*

The equation of motion for a structure can be expressed as

$$\mathbf{M}\{\ddot{u}(t)\} + \mathbf{C}\{\dot{u}(t)\} + \mathbf{K}\{u(t)\} = \{F(t)\} \tag{7}$$

where $\{u(t)\}, \{\dot{u}(t)\}, \{\ddot{u}(t)\}$ are the nodal displacement, velocity and acceleration vectors, respectively; **M**, **K**, **C** are the system mass, stiffness and damping matrices, respectively; $\{F(t)\}$ is a nodal force vector.

It is reasonable to assume that structural damage is due to the damage of elementary stiffness, regardless of the damage of elementary mass. The degree of damage of the $j$-th structure element can be quantified by a value $\alpha_j$ ($\alpha_j \in [0,1]$) (Perera and Ruiz 2008). Herein, $\alpha_j = 1$ represents that the element is intact and $\alpha_j = 0$ denotes that the element is completely damaged. Therefore, the global stiffness matrix of the damaged structure can be written as follows

$$\mathbf{K} = \sum_{j=1}^{n} (1 - \alpha_j)\mathrm{k}_j^e, L_b \le \alpha_j \le U_b \tag{8}$$

where $\mathrm{k}_j^e$ is the stiffness matrix of the $j$th element; $n$ is the total number of finite elements, the same as the number of decision variables in CMFOA; $L_b$ and $U_b$ are the upper and lower limits of damage parameters, respectively.

#### *2.2.2 Objective function*

A damage in a structure usually causes a change in its system parameters, and thus leads to a change in structural dynamic responses. The responses are usually calculated by

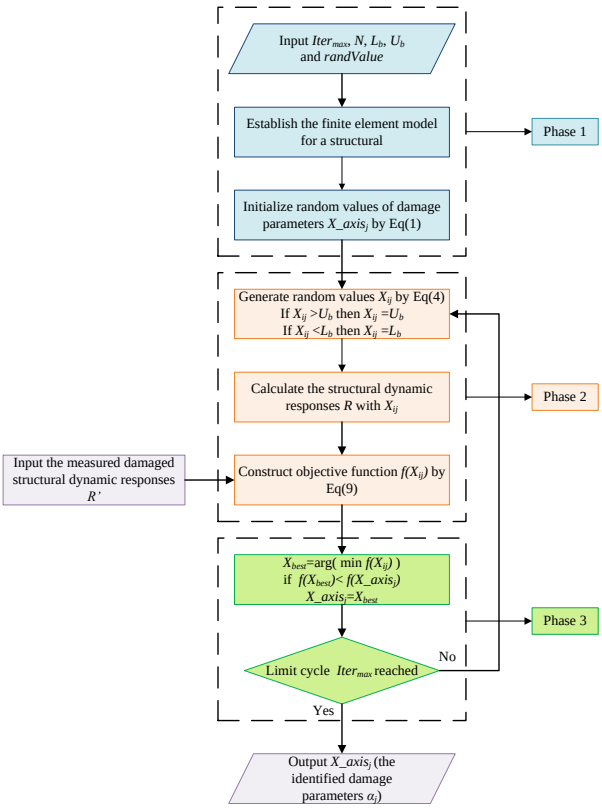


Fig. 2 Flow chart of structural damage identification using CMFOA

Newmark-$\beta$ method. In order to identify the damage, an objective function can be constructed by minimizing the differences between the calculated and measured values of the structural dynamic responses and can be written as

$$f(\alpha_j) = \frac{1}{2}\sum_{p=1}^{nm}\sum_{q=1}^{nt}\left(R'_{pq} - R_{pq}\right)^T\left(R'_{pq} - R_{pq}\right), j = 1,2,\ldots,n \tag{9}$$

where $nm$ and $nt$ are the number of measured points and sampling points in the time history, respectively; $R$ and $R'$ are the calculated and measured values of responses, respectively. The resulting of damage parameter $\alpha_j$ is finally obtained can be obtained under the condition that the objective function $f(\alpha_j)$ satisfies given stop criteria.

## 3. Implementation

Fig. 4 shows a flow chart of the implementation of the methodology in Section 2 for structural damage identification using CMFOA, which consists of three phases: (1) initialization of the problem parameters, (2) osphresis foraging phase, and (3) vision foraging phase. Detailed procedures are summarized as follows

Step 1. Input the maximum iterative number $Iter_{max}$, the fruit fly swarm population $N$, the lower bound $L_b$ and upper bound $U_b$ of swarm location, and *randValue*;

Step 2. Establish the finite element model for a structure;

Step 3. Initialize a random value $X\_axis_j$ by Eq. (1);

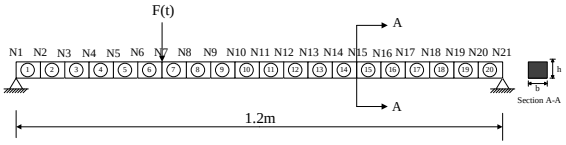


Fig. 3 Beam model

Step 4. Generate $X_{ij}$ randomly around the present fruit fly swarm position by Eq. (4), which indicates a new solution of the structural damage element and its parameters.

Step 5. Input initial nodal displacement, velocity and acceleration, and the external excitation $\{F(t)\}$, and then calculate structural dynamic responses $R$ with the generated damage parameters $X_{ij}$ by Newmark-$\beta$ method;

Step 6. Input the measured dynamic response $R'$ of a damaged structure and construct objective function by Eq. (9);

Step 7. Find $X_{best}$ among the fruit fly swarm and choose $X_{best}$ to be the $X\_axis_j$ in the next iteration if $f(X_{best})< f(X\_axis_j)$;

Step 8. Repeat Steps 4-7 until the maximum iterative number $Iter_{max}$ is reached;

Step 9. Output $X\_axis_j$ as the identified damaged parameters $\alpha_j$ of the structure.

## 4. Numerical examples

The performance of CMFOA is verified in this section by identifying either single damage or multiple damages in a simply supported beam and a cantilevered plate. The maximum iterative number $Iter_{max}$ is taken as 500 for the case with a single element damage and as 2000 for the case with multiple element damages, respectively. The population $N$ is taken as 180. The upper and lower limits of damage parameters $U_b$ and $L_b$ are set as 1 and 0.5, respectively. The parameters of Newmark-$\beta$ method $\gamma$ and $\beta$ are taken as 0.5 and 0.25, respectively. The initial nodal displacement, velocity and acceleration of are all set as zeros. The damage identification method using the basic FOA is utilized as well, serving as a comparison for the present method in terms of the effectiveness, efficiency and accuracy either without or with noise.

### *4.1 A simply supported beam*

Fig. 3 shows the numerical model of a simply supported beam, which has been employed for the structural damage detection using improved PSO (Wei *et al.* 2012). The beam is 1.2 m long with a cross section of 0.05×0.006 m$^2$. The finite element model of the beam has 21 nodes and 20 elements, and the node and element numbers are denoted by Arabic numbers with an initial N and inside a circle, respectively. The material properties of the beam are given as follows: Young's modulus $E = 70\text{GPa}$, mass density $\rho = 2.70 \times 10^3$ kg/m$^3$ and Poisson's ratio $\mu = 0.33$.

Assume that an impulsive force is applied at the seventh nodes with magnitudes

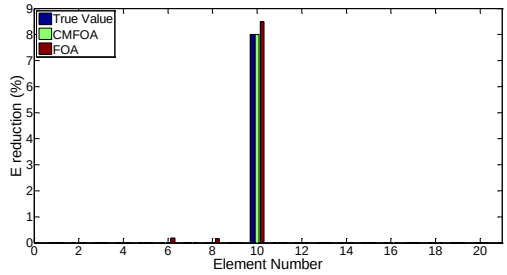


(a) Without noise

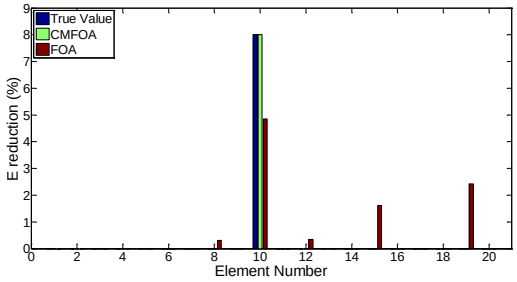


(b) With 2% noise

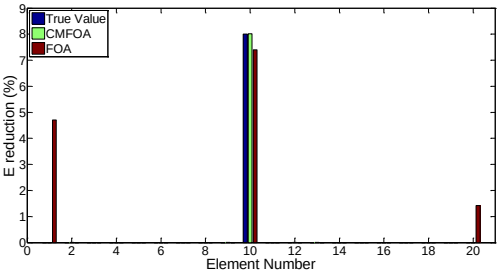


(c) With 5% noise

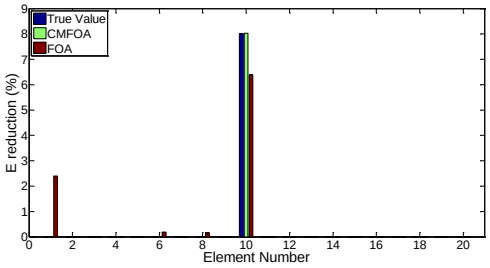


(d) With 10% noise

Fig. 4 Identified results of the beam with a single damage under various noise conditions

$$\mathrm{F(t)} = \begin{cases} 100(t-0.02)N & (0.02 \le t \le 0.04) \\ 100(0.06-t)N & (0.04 \le t \le 0.06). \\ 0 & (t < 0.02 \; or \; t > 0.06) \end{cases} \tag{10}$$

The acceleration responses at N3, N6, N14 and N19 are calculated as the "measured" responses, and then used as input data to construct the objective equation, that is Eq. (9). The time duration of measurement lasts for 6.0 second and the sampling frequency is 200 Hz. To consider measurement noise in the laboratory condition, a Gaussian noise with amplitudes of 2%, 5% and 10% are imported in the course of identification. The following three cases will be considered: one case is with a single element damage and the other one is with multiple element damages.

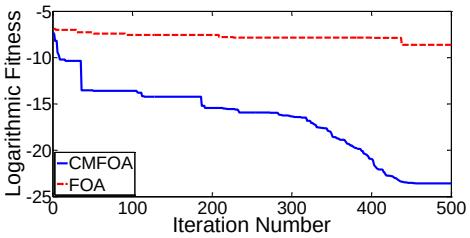


(a) Without noise

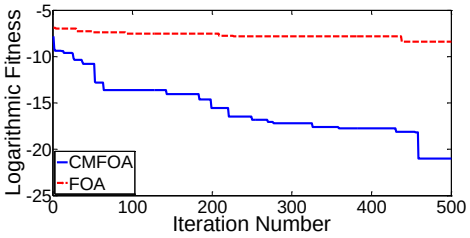


(b) With 2% noise

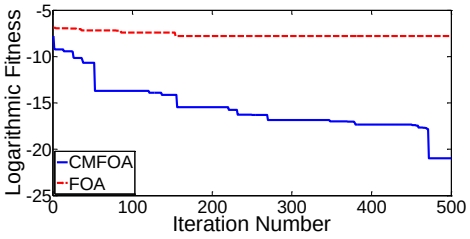


(c) With 5% noise

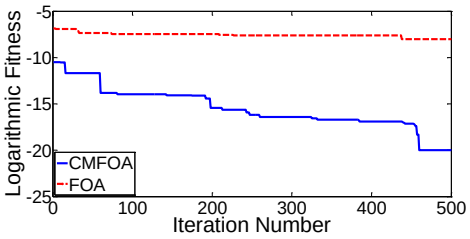


(d) With 10% noise

Fig. 5 Iterative processes of logarithmic fitness values of the beam with a single damage under various noise conditions

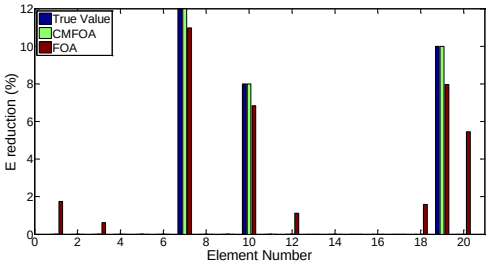


(a) Without noise

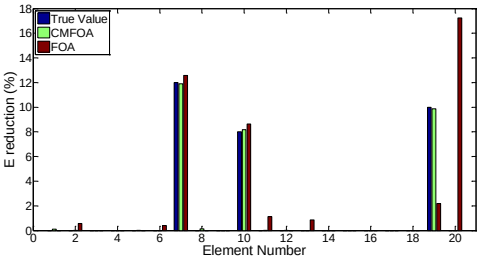


(b) With 2% noise

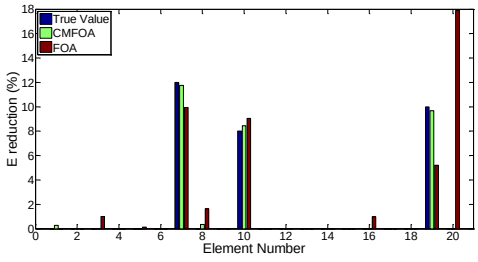


(c) With 5% noise

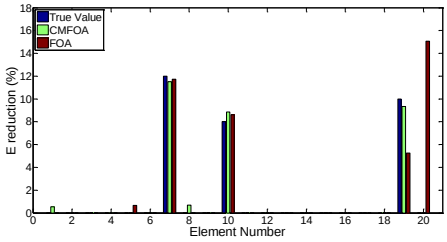


(d) With 10% noise

Fig. 6 Identified results of the beam with three element damages under various noise conditions

#### *4.1.1 Case 1: Identification of a single element damage for beam model*

In this case, it is assumed that the tenth element has 8% reduction in its element stiffness. Fig. 4 shows the damage identification results under various noise conditions. In the figure, the colourized bars indicate the identified reductions of Young's modulus at different elements along the beam, among which blue bar is the true value, and light green and red bars represent the results by identification methods using CMFOA and FOA, respectively. In the noise-free condition, as shown in Fig. 4(a), CMFOA is able to accurately detect the stiffness reduction at the tenth element, while the result with FOA is a bit over-estimated and minor defects at the sixth and eighth elements are falsely identified. When the measured responses are polluted by noise, as shown in Figs. 4(b)-4(d), CMFOA can still obtain quite desirable identification results, while FOA tends to detect lower values of stiffness reduction at the tenth element with several false elements being identified. The degree of stiffness reduction of those falsely identified elements increases quite dramatically if the noise is under consideration. In summary, the present method has better accuracy performance than FOA, regardless of the noise.

Fig. 5 shows the corresponding iterative processes of fitness values in a logarithmic form for CMFOA and FOA. It can be observed that the former converges to the global optimal solution with higher accuracy and faster convergence speed than the latter no matter in the condition with or without noise. It also shows that FOA is easy to bring premature convergence and to be trapped in the local optimal solution because of the inherent deficiency of using the uniformly distributed random function. While the convergence ability of the present method is significantly improved. This is due to the usage of the normal cloud model in the osphresis phase, which is able to take both the randomness and fuzziness features of the fruit fry swarm

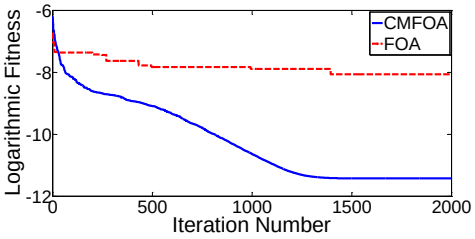


(a) Without noise

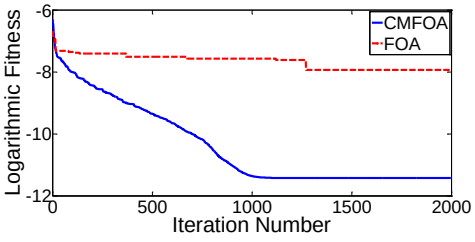


(b) With 2% noise

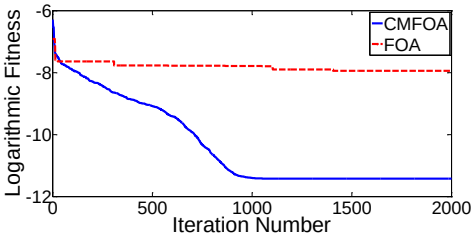


(c) With 5% noise

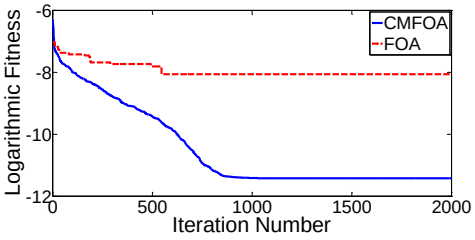


(d) With 10% noise

Fig. 7 Iterative processes of logarithmic fitness values of the beam with three element damages under various noise conditions

foraging behavior. In addition, the present method can still obtain excellent convergence as the amplitude of noise increases.

#### *4.1.2 Case 2: Identification of multiple element damages for beam model*

Multiple element damages in the beam model are considered in this case. It is assumed that the seventh, tenth and nineteenth elements have 10%, 8% and 12% reduction in their corresponding elemental stiffness, respectively, that is, $\alpha_7 = 0.9$, $\alpha_{10} = 0.92$ and $\alpha_{19} = 0.88$. Both noise-free and noise-contaminated conditions are considered as well.

Fig. 6 shows the identified results of the beam with damages in the seventh, tenth and nineteenth elements under the condition with and without noise. In the noise-free case, CMFOA is able to accurately identified the stiffness reduction at the three elements, while FOA detect lower values in these three elements and falsely identified not very small defects in the first (1.8%), third (0.6%), twelfth (1.1%), eighteenth (1.6%) and twentieth elements (5.5%). In the case with noise, as presented in Figs. 6(b)-(d), CMFOA is still able to obtain satisfiable results, although minor defects (less than 0.5%) are falsely detected and this deficiency tends to increase as the increase of noise level. For FOA, its general performance is rather poor and a significant fault damage is found at the twentieth element. This maybe because the FOA falls into a local optimal solution from which the present method can escape.

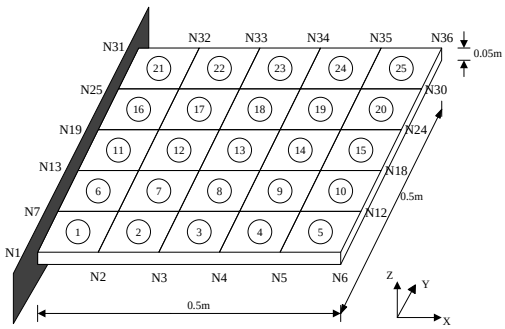


Fig. 8 Plate model

The iterative processes of logarithmic best fitness values of the two methods are illustrated in Fig. 7. Under the noise-free condition, it is observed that the evolution curve of the FOA drops down significantly in the early search stage, and soon becomes much steady and almost a straight line finally. For the curve of the present method, it descends with a relatively low speed in the early search stage, and continues to decrease with an almost linear convergence rate, and starts to become flat at about 1300 steps. Similar trends of the two curves can be found in Figs. 7(b)-(d) under the noise-contaminated conditions. This phenomenon suggests that the present method can converge to the global optimal solution while the FOA is trapped to a local one, and confirms the judgement of accuracy performance between the two methods in Fig. 6. Thus, it can be concluded that the present method significantly outperforms the basic FOA for damage identification in the beam model with multiple damages.

### *4.2 A cantilevered plate*

The present method is also used to identify the damage in a cantilevered plate, which has been utilized for the structural damage identification using finite element model updating in time domain (Fu *et al.* 2013). The plate in size of 500×500×50 $mm^3$ is shown in Fig. 8. The finite element model of the plate has 36 nodes and 25 elements. The material properties of the plate are given as follows: Young's modulus $E = 210\text{GPa}$, mass density $\rho = 7.80 \times 10^3\ \text{kg/m}^3$ and Poisson's ratio $\mu = 0.3$.

An impulsive force is assumed to apply at N22 with magnitudes

$$\text{F(t)} = \begin{cases} 200(t-0.02)N & (0.02s \le t \le 0.04s) \\ 200(0.06-t)N & (0.04s \le t \le 0.06s) \\ 0 & (t < 0.02s \ or \ t > 0.06s) \end{cases} \quad (11)$$

The acceleration responses at N10, N15, N23, and N29 are calculated by Newmark-$\beta$ method, and are later used to

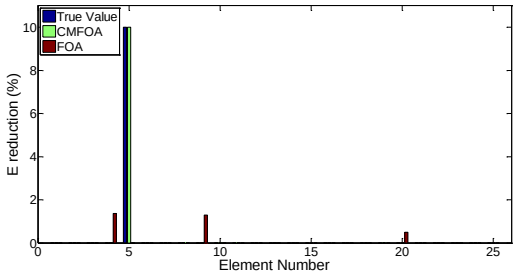


(a) Without noise

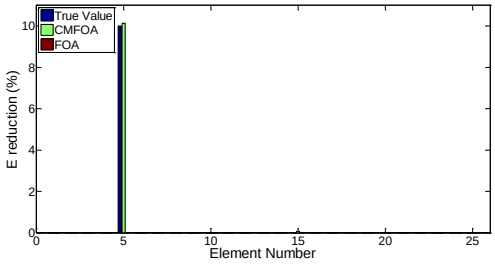


(b) With 2% noise

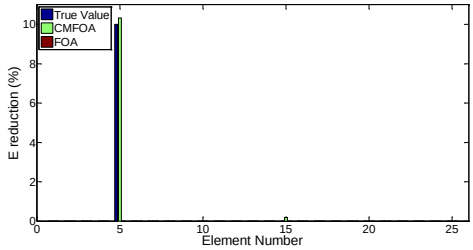


(c) With 5% noise

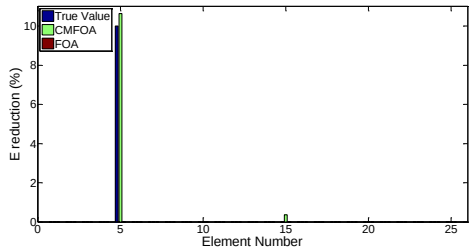


(d) With 10% noise

Fig. 9 Identified results of the plate with a single damage under various noise conditions

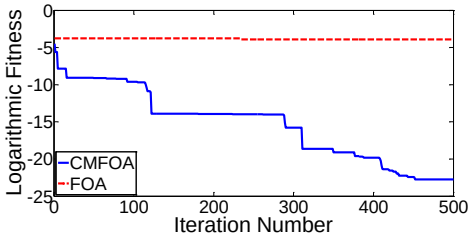


(a) Without noise

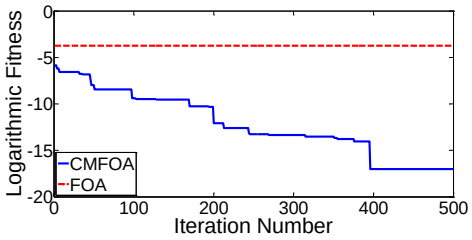


(b) With 2% noise

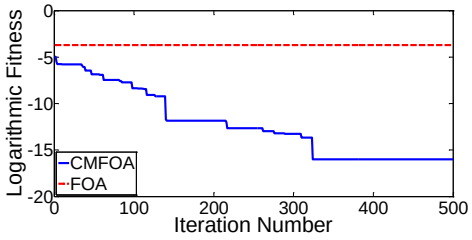


(c) With 5% noise

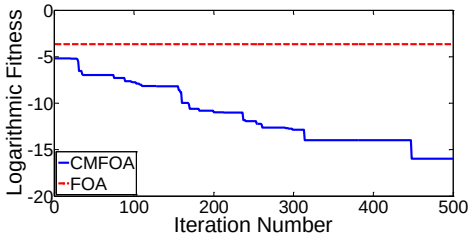


(d) With 10% noise

Fig. 10 Iterative processes of logarithmic fitness values of the plate with a single damage under various noise conditions

identify the damage in the plate. A sampling frequency of 1000 Hz and a short time duration of 2 second are adopted in this numerical example. Again, the cases with single damage and multiple damages are studied respectively.

#### *4.2.1 Case 1: Identification of a single damage*

In this case, a single damage is assumed in the fifth element of the plate model, with 10% reduction in its element stiffness. The actual reduction and the damage identification results of the plate for the condition without and with 2%, 5% and 10% noise are presented in Fig. 9. In the case without noise, as shown in Fig. 9(a), the present method accurately detects the elementary damage without any faults being found, whereas FOA fails to identify any damage in the fifth element and gives extra damages in the fourth, ninth and twentieth elements by mistake. In the cases with noise, fairly accurate results can be observed for the present method, although a minor defect is falsely found in the fifteenth element. The accuracy slightly decreases and the minor defect increases a bit, as the amplitude of noise increases. By contrast, FOA is unable to detect any damage at all under the noise-contaminated conditions.

The iterative processes of fitness values in a logarithmic form for the two methods are shown in Fig. 10. From these figures, it can be recognized that the convergence of the present method is much superior to its counterpart under both noise-free and noise-contaminated conditions. It should be noted that there's almost no convergence of the basic FOA, implying that it almost lost its ability for detecting damage in this case. This confirms its failure identification in Fig. 9. As the amplitude of noise increases, CMFOA can still obtain excellent convergence.

#### *4.2.2 Case 2: Identification of multiple damages*

In this case, damages are assumed to appear in the

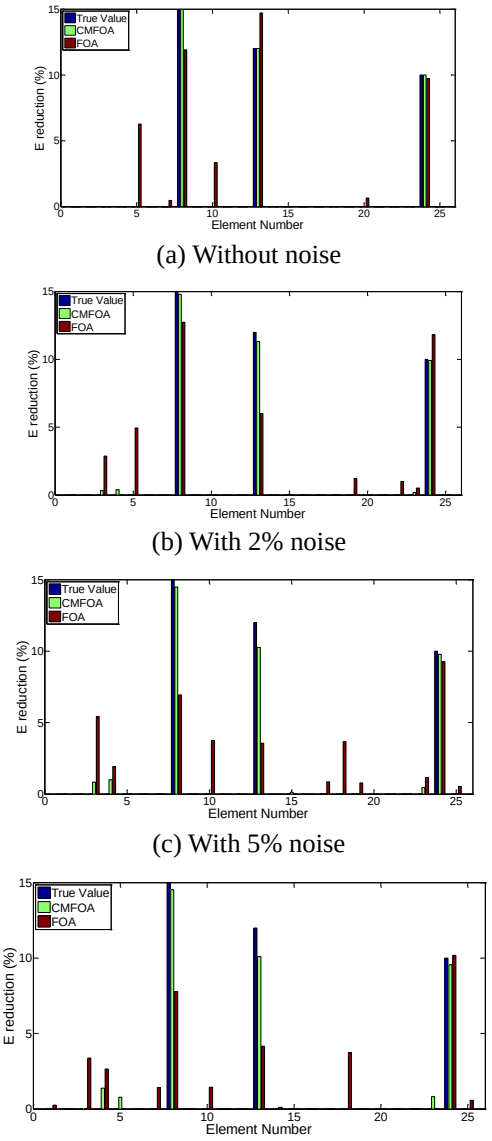


(a) Without noise

(b) With 2% noise

(c) With 5% noise

(d) With 10% noise

Fig. 11 Identified results of the plate with three element damages under various noise conditions

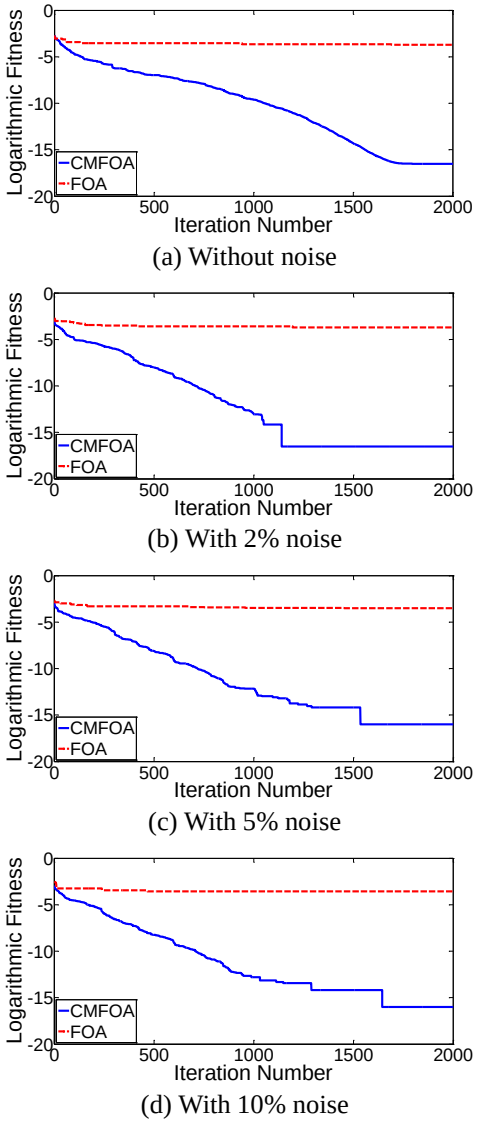


(a) Without noise

(b) With 2% noise

(c) With 5% noise

(d) With 10% noise

Fig. 12 Iterative processes of logarithmic fitness values of the plate with three element damages under various noise conditions

eighth, thirteenth and twenty-fourth elements, with 15%, 12% and 10% reduction in their corresponding elemental stiffness respectively, that is, $\alpha_8 = 0.9$, $\alpha_{13} = 0.92$ and $\alpha_{24} = 0.88$. Fig. 11 shows the identified stiffness reduction results by the CMFOA and the basic FOA. Under the noise-free condition, CMFOA is able to accurately identified the stiffness reduction in three damaged elements without any faults being detected. The accuracy of the CMFOA is compromised by noise, and its results tend to increasingly lower than the true values with several wrongly identified damages as the increase of noise level. Unlike the case of a single damage for the plate model (Section 4.2.1), FOA manages to find the three damaged elements although quite diverse extra elements are falsely detected and their amount of stiffness reduction is relatively large. The reason lies in an inherent feature of the basic FOA: it changes all the decision variants ($\alpha_j$, j = 1, 2, …, 25 in this plate model) of the swarm location when producing a new location. In other words, the basic FOA has better performance in the case with multiple damages than the case with one damage only. This can be confirmed in the beam model that the convergence rate in the early search stage in Fig. 7 is much higher than that in Fig. 5. By contrast, the CMFOA randomly chooses one decision variant only to generate a new solution, as given in Eq. (4), thus it is more flexible to suit with both cases with a single damage and multiple damages.

The iterative processes of logarithmic best fitness values of the CMFOA and the FOA are illustrated in Fig. 12. The evolution curve of the CMFOA in this case has similar trends as the case of multiple damages in the beam model (Fig. 7): it decreases very fast in the early search stage, and soon drops down with almost a linear descend rate, and converges to the global optimal solution at the end of iteration. For the curve of FOA, its overall convergence, similar to the curve features in Fig. 10, is poor, but a short convergence stage is still observed in the early process. This

is because, as aforementioned, the basic FOA is superior in the case with multiple damages than the case with one damage only.

## 5. Conclusions

In this paper, a cloud model based fruit fly optimization algorithm was implemented for structural damage identification problem. Two damage identification examples on a simply supported beam and a cantilevered plate were studied under conditions without and with noise. Major findings are listed as follows:

- Under the condition with multiple damages, FOA tends to be sensitive to artificial measurement noise in the beam model and fails to obtain any optimal solution in the plate model, whereas CMFOA has excellent performances and is not sensitive to noise.
- For the condition with multiple damages, CMFOA is able to obtain better solutions than FOA in both the beam model and the plate model.
- CMFOA can always converge the global optimal solution while the basic FOA is easy to be trapped to a local one.

The CMFOA is generally superior to the FOA in terms of effectiveness, efficiency and accuracy for structural damage identification.

## Acknowledgments

This work is supported by a research grant from National Key Research and Development Program of China (project No. 2017YFC1500400), the Guangdong Province Science and Technology Program (2016A020223006) and the Fundamental Research Funds for the Central Universities (171gjc42). Such financial aids are gratefully acknowledged.

## References

Bakhtiari-Nejad, F., Rahai, A. and Esfandiari, A. (2005), "A structural damage detection method using static noisy data", *Eng. Struct.*, **27**(12), 1784-1793.

Cao, M., Ye, L., Zhou, L., Su, Z. and Bai, R. (2011), "Sensitivity of fundamental mode shape and static deflection for damage identification in cantilever beams", *Mech. Syst. Sign. Pr.*, **25**(2), 630-643.

Chen, P.W., Lin, W.Y., Huang, T.H. and Pan, W.T. (2013), "Using fruit fly optimization algorithm optimized grey model neural network to perform satisfaction analysis for e-business service", *Appl. Math. Inform. Sci.*, **7**(2), 459-465.

Daei, M. and Mirmohammadi, S.H. (2015), "A flexibility method for structural damage identification using continuous ant colony optimization", *Multidiscipl. Model. Mater. Struct.*, **11**(2), 186-201.

Ding, Z.H., Huang, M. and Lu, Z.R. (2016), "Structural damage detection using artificial bee colony algorithm with hybrid search strategy", *Swarm Evol. Comput.*, **28**, 1-13.

Fu, Y.Z., Lu, Z.R. and Liu, J.K. (2013), "Damage identification in plates using finite element model updating in time domain", *J. Sound Vibr.*, **332**(26), 7018-7032.

Gao, F. and Lu, Y. (2009), "An acceleration residual generation approach for structural damage identification", *J. Sound Vibr.*, **319**(1-2), 163-181.

Guo, H. (2017), "Structural multi-damage identification based on strain energy and micro-search artificial fish swarm algorithm", *J. Vibroeng.*, **19**(5), 3255-3270.

Hosseinzadeh, A.Z., Amiri, G.G. and Koo, K.Y. (2015), "Optimization-based method for structural damage localization and quantification by means of static displacements computed by flexibility matrix", *Eng. Optim.*, **48**(4), 543-561.

Kim, J.T., Ryu, Y.S., Cho, H.M. and Stubbs, N. (2003), "Damage identification in beam-type structures: Frequency-based method vs mode-shape-based method", *Eng. Struct.*, **25**(1), 57-67.

Li, J. and Hao, H. (2016), "A review of recent research advances on structural health monitoring in Western Australia", *Struct. Monitor. Mainten.*, **3**(1), 33-49.

Li, J., Hao, H. and Lo, J.V. (2015), "Structural damage identification with power spectral density transmissibility: Numerical and experimental studies", *Smart Struct. Syst.*, **15**(1), 15-40.

Li, S. and Lu, Z.R. (2015), "Multi-swarm fruit fly optimization algorithm for structural damage identification", *Struct. Eng. Mech.*, **56**(3), 409-422.

Majumdar, A., Nanda, B., Maiti, D.K. and Maity, D. (2014), "Structural damage detection based on modal parameters using continuous ant colony optimization", *Adv. Civil Eng.*, 110-123.

Nobahari, M., Ghasemi, M.R. and Shabakhty, N. (2017), "Truss structure damage identification using residual force vector and genetic algorithm", *Steel Compos. Struct.*, **25**(4), 485-496.

Pan, Q.K., Sang, H.Y., Duan, J.H. and Gao, L. (2014), "An improved fruit fly optimization algorithm for continuous function optimization problems", *Knowl-Bas. Syst.*, **62**(5), 69-83.

Pan, W.T. (2011), "A new evolutionary computation approach: Fruit fly optimization algorithm", *Proceedings of the Conference on Digital Technology and Innovation Management*, Taipei, Taiwan.

Pan, W.T. (2012), "A new fruit fly optimization algorithm: Taking the financial distress model", *Knowl-Bas. Syst.*, **26**(2), 69-74.

Pan, W.T. (2013), "Using modified fruit fly optimization algorithm to perform the function test and case studies", *Connect. Sci.*, **25**(2-3), 151-160.

Patel, S., Peacock, S.M., McKinley, R.K., Clark Carter, D. and Watson, P.J. (2011), "Aircraft failure detection and identification over an extended flight envelope using an artificial immune system", *Aeronaut. J.*, **115**(1163), 43-55.

Perera, R. and Ruiz, A. (2008), "A multistage FE updating procedure for damage identification in large scale structural based on multiobjective evolutionary optimization", *Mech. Syst. Sign. Pr.*, **22**(4), 970-991.

Saada, M.M., Arafa, M.H. and Nassef, A.O. (2013), "Finite element model updating approach to damage identification in beams using particle swarm optimization", *Eng. Optim.*, **45**(6), 677-696.

Sun, H., Luş, H. and Betti, R. (2013), "Identification of structural models using a modified artificial bee colony algorithm", *Comput. Struct.*, **116**(1), 59-74.

Sun, Z.G., Chen, Y.F., Shao, Y., Shi, J. and Li, Y.N. (2014), "Model test study on damage identification for suspension bridges", *Eng. Mech.*, **31**(6), 132-137.

Teixeira, J.S., Stutz, L.T., Knupp, D.C. and Neto, A.J.S. (2016), "Structural damage identification via time domain response and Markov Chain Monte Carlo method", *Inv. Probl. Sci. En.*, **25**(6), 1-27.

Wang, J.Y. and Ni, Y.Q. (2015), "Refinement of damage

identification capability of neural network techniques in application to a suspension bridge", *Struct. Monitor. Maint.*, **2**(1), 77-93.

Wei, J.J. (2011), "Comparison of analytical approaches to tall building structural damage identification based on measured dynamic characteristics", *Appl. Mech. Mater.*, 105-107, 1081-1086.

Wei, Z., Liu, J. and Lu, Z. (2012), "Structural damage detection using improved particle swarm optimization", *Ksii T. Internet Inf. Syst.*, **6**(18), 4733-4746.

Wu, L., Zuo, C. and Zhang, H. (2015), "A cloud model based fruit fly optimization algorithm", *Knowl-Bas. Syst.*, **89**(C), 603-617.

Xia, Y., Hao, H., Brownjohn, J.M.W. and Xia, P.Q. (2002), "Damage identification of structures with uncertain frequency and mode shape data", *Earthq. Eng. Struct. D.*, **31**(5), 1053-1066.

Xu, H.J., Ding, Z.H., Lu, Z.R. and Liu, J.K. (2015), "Structural damage detection based on chaotic artificial bee colony algorithm", *Struct. Eng. Mech.*, **55**(6), 1223-1239.

Yuan, X., Dai, X., Zhao, J. and He, Q. (2014), "On a novel multi-swarm fruit fly optimization algorithm and its application", *Appl. Math. Comput.*, **233**(3), 260-271.

Zhang, L.T., Li, Z.X. and Fei, Q.G. (2007), "Study on structural damage identification using acceleration data in time domain", *J. Vibr. Shock*, **26**(9), 138-141.

Zhu, H.P., Mao, L. and Weng, S. (2014), "A sensitivity-based structural damage identification method with unknown input excitation using transmissibility concept", *J. Sound Vibr.*, **333**(26), 7135-7150.

*CC*